Supporting Information:

Temperature-Sensitive Localized Surface Plasmon Resonance of α-NiS Nanoparticles

Rasmus Himstedt[a,b], Dirk Baabe[c], Christoph Wesemann[a,b], Patrick Bessel[a,b], Dominik Hinrichs[a,b], Anja Schlosser[a,b], Nadja C. Bigall[a,b,d], and Dirk Dorfs[a,b,d]*

[a]R. Himstedt, C. Wesemann, P. Bessel, D. Hinrichs, A. Schlosser, N. C. Bigall, and D. Dorfs
Institute of Physical Chemistry and Electrochemistry, Leibniz Universität Hannover, Callinstraße 3A, 30167 Hannover, Germany

[b]R. Himstedt, C. Wesemann, P. Bessel, D. Hinrichs, A. Schlosser, N. C. Bigall, and D. Dorfs
Laboratory of Nano and Quantum Engineering, Leibniz Universität Hannover, Schneiderberg 39, 30167 Hannover, Germany

[c]D. Baabe
Institut für Anorganische und Analytische Chemie, Technische Universität Braunschweig, Hagenring 30, 38106 Braunschweig, Germany

[d]N. C. Bigall and D. Dorfs
Cluster of Excellence PhoenixD (Photonics, Optics, and Engineering – Innovation Across Disciplines), Leibniz Universität Hannover, 30167 Hannover, Germany

E-Mail: dirk.dorfs@pci.uni-hannover.de

TEM analysis and UV-Vis absorbance spectra of Au nanocrystals (AuNCs)

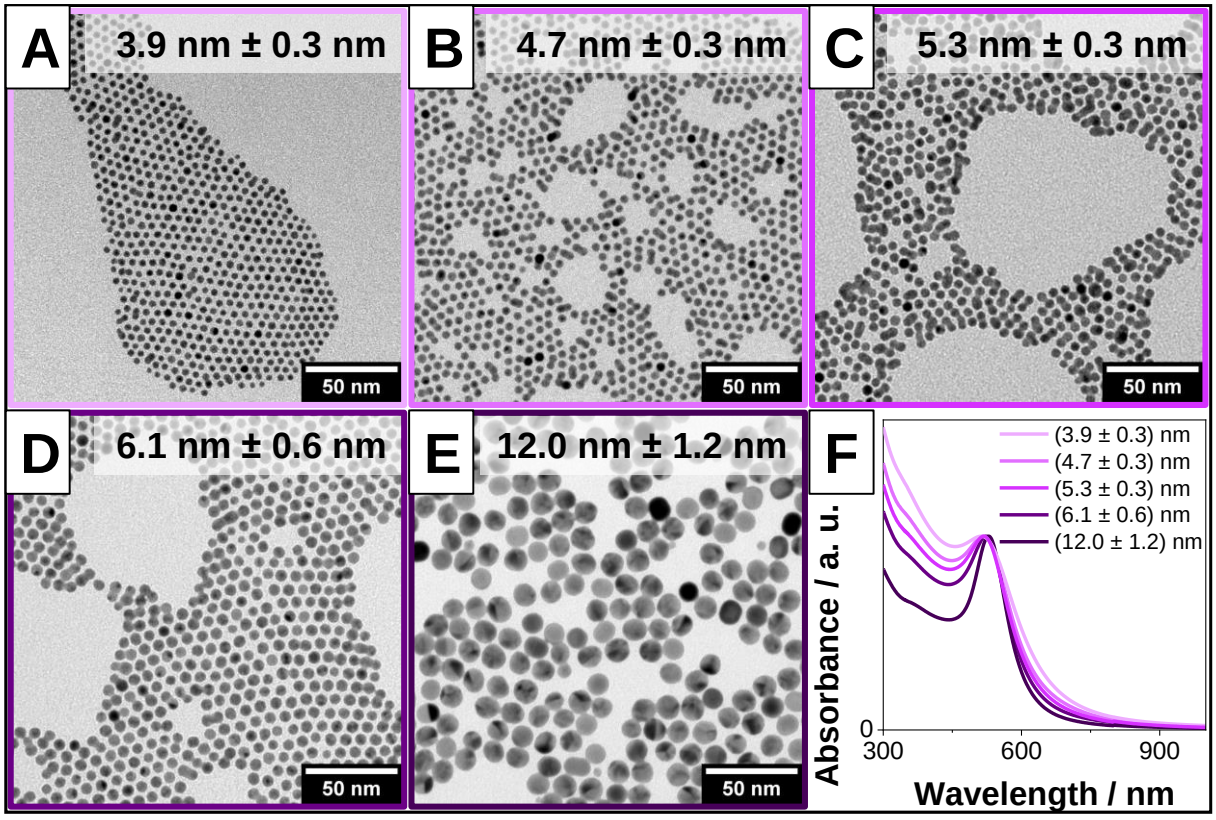

Figure S1. TEM overview images showing Au nanocrystals of different sizes (A-E) and the corresponding UV-Vis absorbance spectra of the same samples. The spectra have been normalized to the respective localized surface plasmon resonance (LSPR) maximum. Monodisperse particles could be obtained in all cases, while the LSPR maximum is slightly shifted towards longer wavelengths and gets sharper with an increasing diameter of the AuNCs.

XRD analysis of Au-NiS core-shell nanoparticles

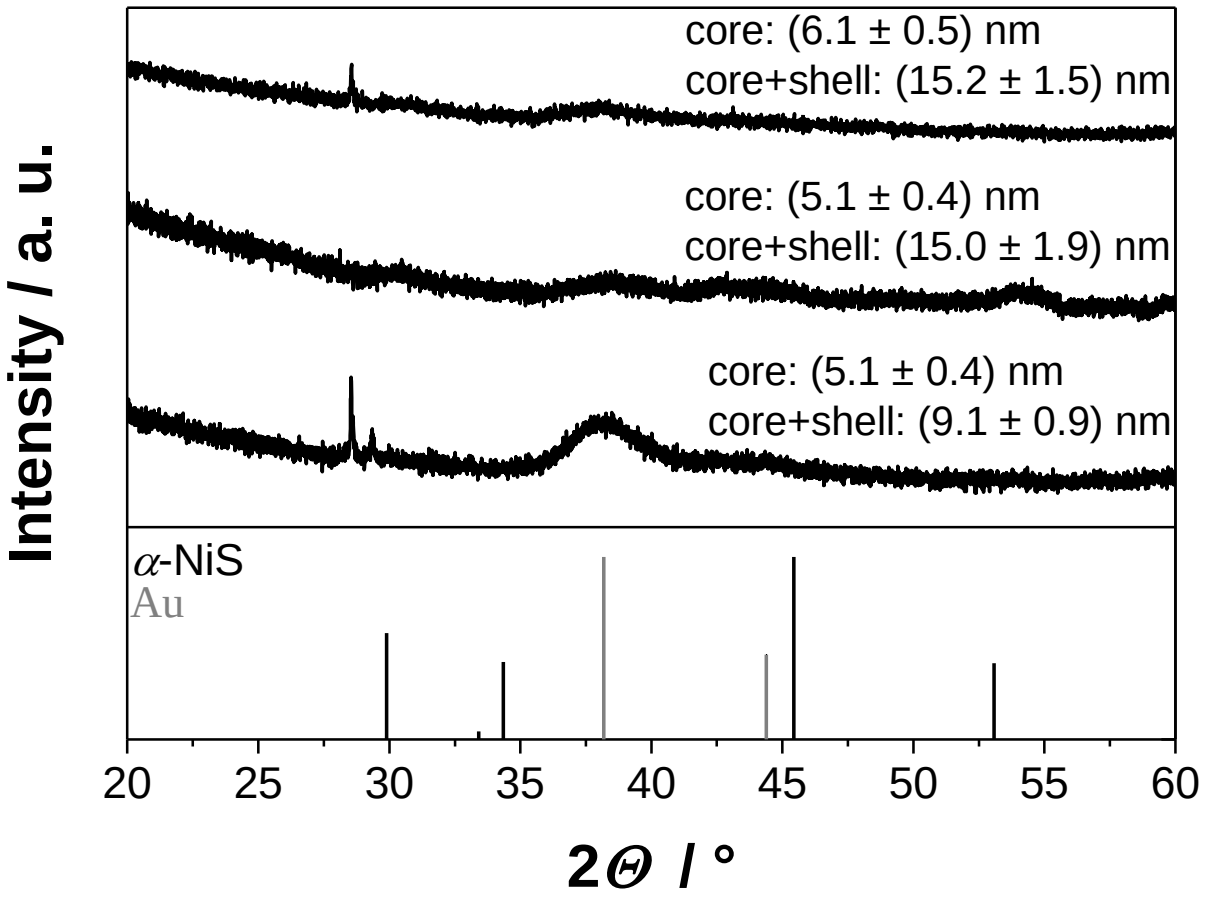

Figure S2. X-ray diffractograms of different Au-NiS samples. The α-NiS and Au references are PDF card # 03-065-0395 and 03-065-2870, respectively. The obtained reflections are significantly broadened due to the small size of the crystallites. The small and rather sharp reflections visible below 30° (2θ) are due to a slight contamination of the measurement device and are not caused by the sample.

Optical analysis of Au-NiS core-shell nanoparticles

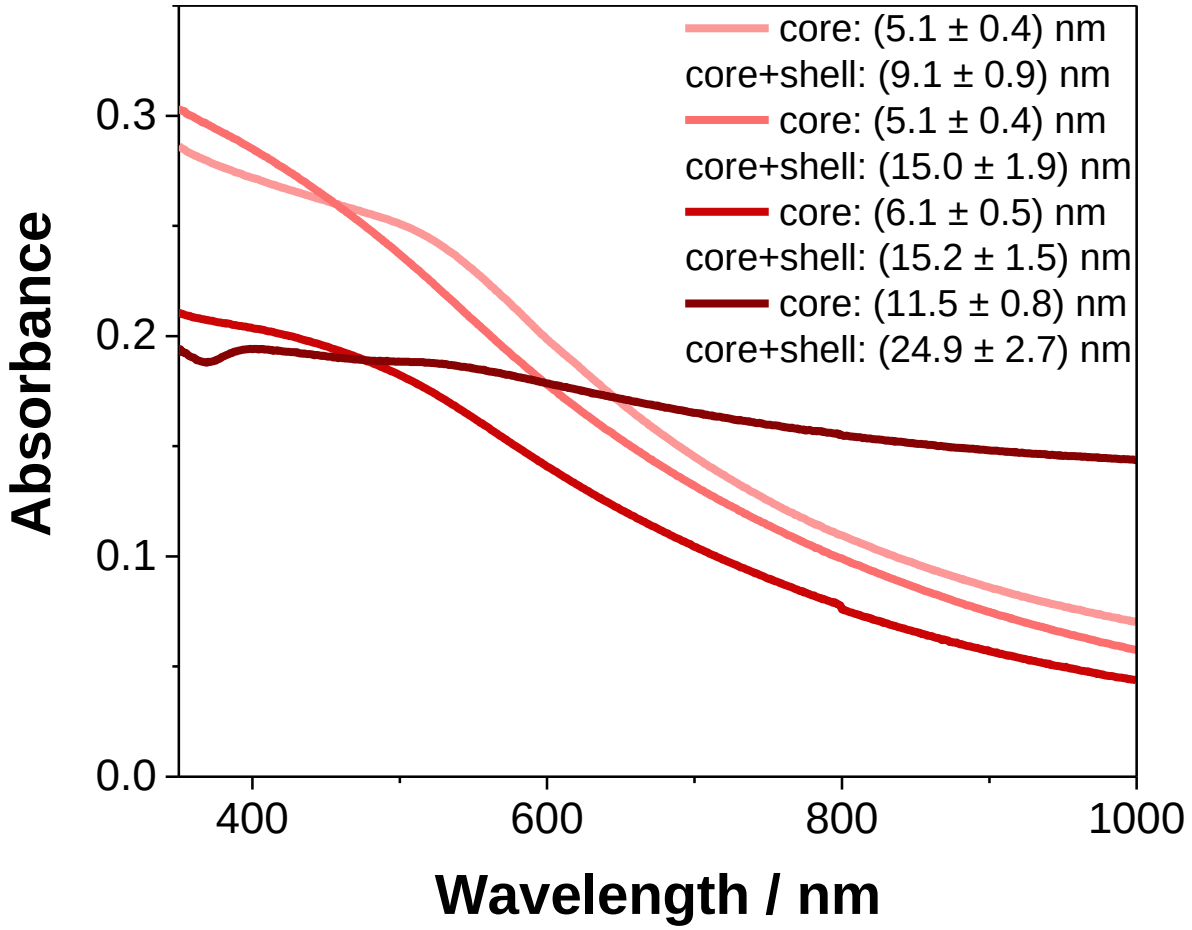

Figure S3. UV-Vis absorbance spectra of the different Au-NiS samples. Compared to the spectra of the core particles in Figure S1 the LSPR maximum of the core-shell nanoparticles is hypsochromically shifted towards the LSPR position of pure *α*-NiS particles (see Figure 3 in the main text) and also broadened significantly due to the stronger damping in the nickel sulfide. The hypsochromic shift is smaller when a thinner shell is grown onto the same cores, which is in line with expectations. The largest investigated core-shell particles show a very broad absorbance, which next to increased scattering is at least in part due to an imperfect colloidal stability of this specific sample. In this case, the very broad spectrum is therefore probably caused by significant aggregation of the large particles in the dispersion.

Full characterization of particles obtained by upscaled syntheses

To obtain enough material for the magnetic susceptibility measurements, the usual synthesis process had to be scaled up seven and ten times for the α-NiS and Au-NiS synthesis, respectively. While the core-shell particles are very similar to the result of the normally scaled synthesis in size and size distribution, the pure α-NiS nanoparticles are slightly larger, less spherical, and more polydisperse (Figure S4 A&C). They are however of the correct NiS phase as can be seen in the XRD pattern (Figure S4 D, the α-NiS and Au references are PDF card # 03-065-0395 and 03-065-2870, respectively). In the case of the core-shell particles, there are, as usual, only very broad and small reflections visible (see Figure S2). The UV-Vis spectra (Figure S4 C) show an LSPR maximum slightly below 500 nm for both particle samples instead of a shoulder at shorter wavelengths as is usually the case (see Figure 3 in the main text). This is most likely caused by aggregation since the particles obtained in the upscaled syntheses are much more concentrated and less colloidally stable in their stock solutions. The very broad absorbance of the α-NiS sample is also in accord with this conclusion since the absorbance at longer wavelengths is probably caused by light scattering processes. Another factor contributing to this could be longitudinal LSPR modes from the strongly elongated particles in the sample visible in the TEM image.

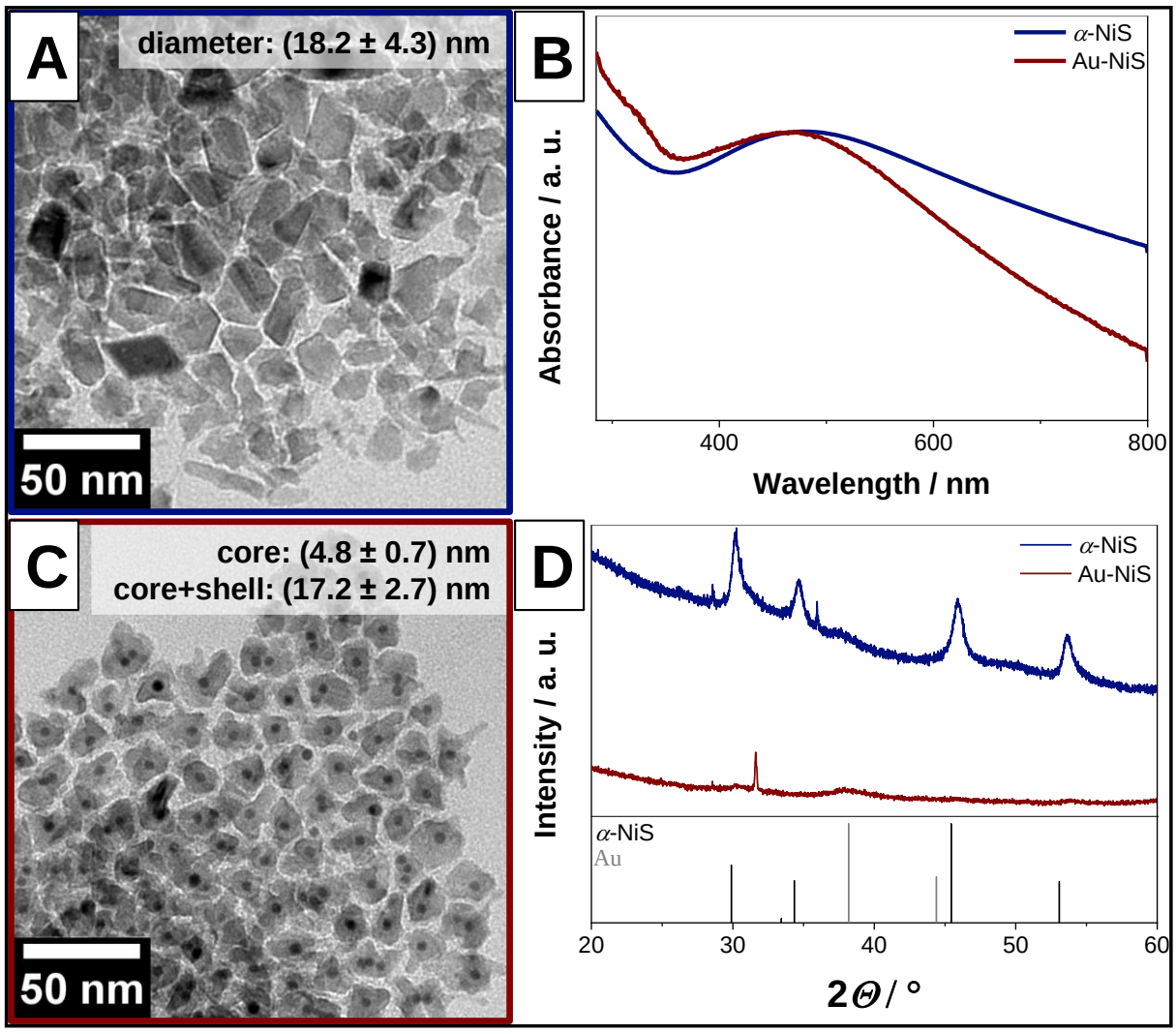

Figure S4. TEM overview images (A&C), UV-Vis absorbance spectra (B), and X-ray diffractograms (D) of α-NiS (blue) and Au-NiS (red) nanoparticles synthesized for the magnetic susceptibility measurements.

Magnetic susceptibility measurements on α-NiS and Au-NiS nanoparticles

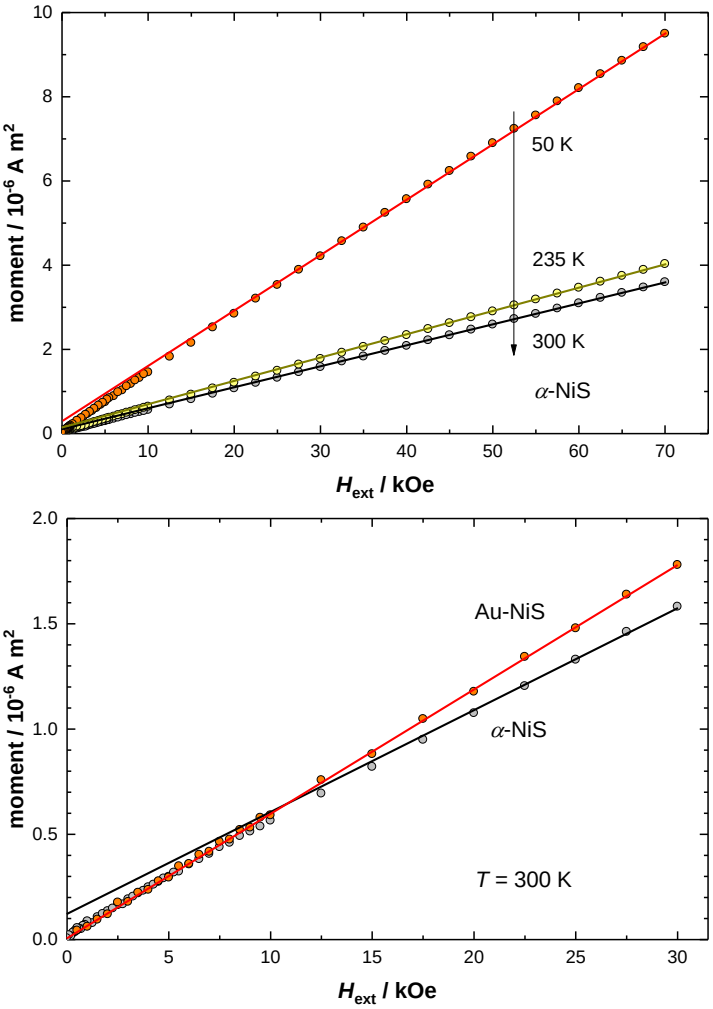

Figure S5. (**Upper panel:**) Isothermal magnetization (*i.e.*, the total magnetic moment of the sample after correction of the diamagnetic contribution of the sample holder) of α-NiS nanoparticles recorded with external magnetic fields between H_{ext} = 0 and 70 kOe at T = 50, 235 and 300 K. The solid lines are to guide the eye. (**Lower panel:**) Isothermal magnetization (*vide supra*) of α-NiS and Au-NiS particles recorded with external magnetic fields between H_{ext} = 0 and 70 kOe, where only the data points with H_{ext} < 30 kOe are shown to emphasize the low magnetic field region and to support the discussion in the main text (regarding a possible ferromagnetic impurity in our α-NiS sample). The α-NiS data shown here are the same data points that are also shown in the upper panel of this figure. The solid lines are to guide the eye.

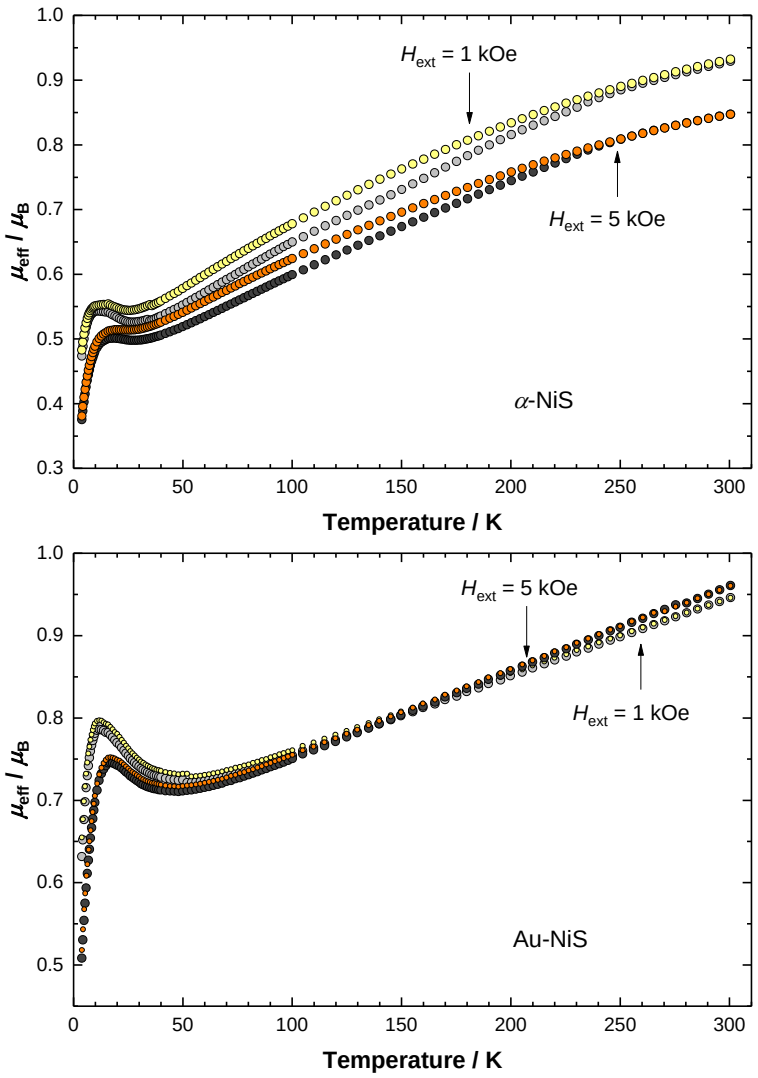

Figure S6. (**Upper panel:**) Effective magnetic moment (per Ni atom) versus temperature of α-NiS nanoparticles recorded between T = 4 and 300 K with external magnetic fields of H_{ext} = 1 and 5 kOe. The measurements were conducted with a field warming sequence after field cooling (yellow and orange symbols) or zero-field cooling (gray and dark gray symbols), respectively. (**Lower panel:**) Effective magnetic moment (per Ni atom) versus temperature of Au-NiS particles recorded between T = 4 and 300 K with external magnetic fields of H_{ext} = 1 and 5 kOe. The measurements were conducted with a field warming sequence after field cooling (yellow and orange symbols) or zero-field cooling (gray and dark gray symbols), respectively.

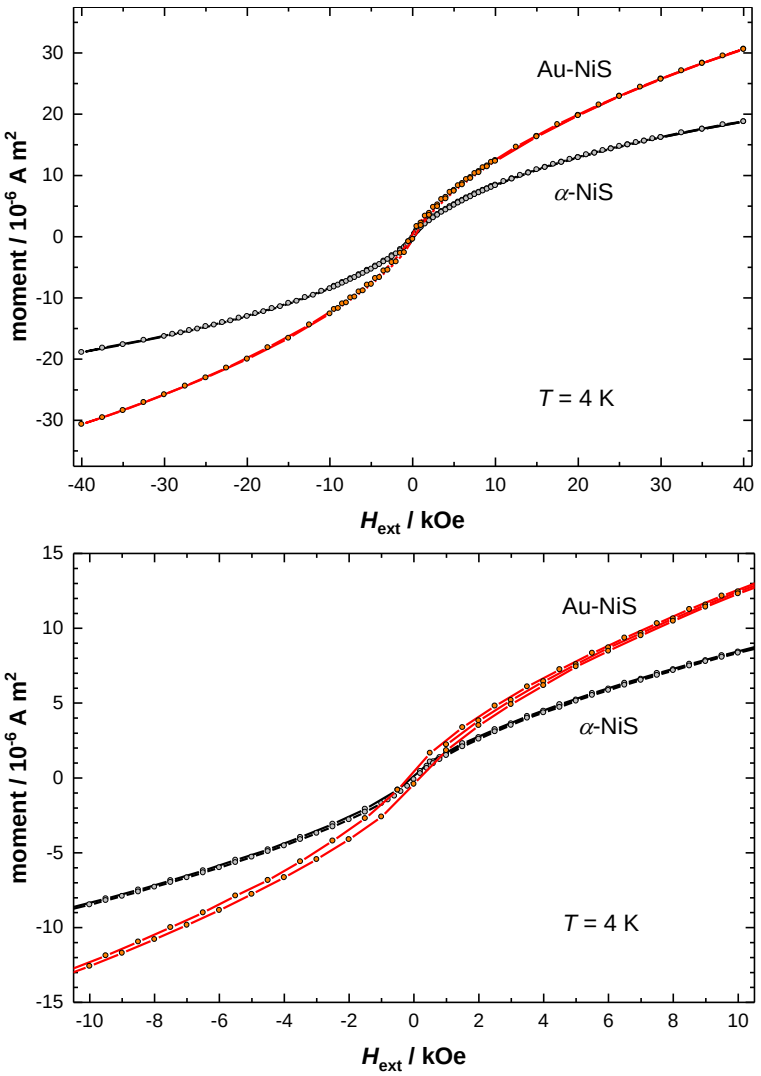

Figure S7. (**Upper panel:**) Isothermal magnetization (*i.e.*, the total magnetic moment of the sample after correction of the diamagnetic contribution of the sample holder) of α-NiS and Au-NiS nanoparticles recorded with external magnetic fields between H_{ext} = -40 and 40 kOe (5 section loop) at T = 4 K. The solid lines are to guide the eye. (**Lower panel:**) The same data as shown in the upper panel of this figure, where only the data points with H_{ext} > -10 kOe and H_{ext} < 10 kOe are shown to emphasize the low magnetic field region and to support the discussion in the main text (regarding the presence of a magnetic field hysteresis in the Au-NiS sample). The solid lines are to guide the eye.